Inorg. Chem. **2008**, *47*, 1779−1786

Forum

Theoretical Studies of O−O Bond Formation in Photosystem II

Per E. M. Siegbahn*

Department of Biochemistry and Biophysics, Arrhenius Laboratory, Stockholm University, SE-106 91 Stockholm, Sweden

Received June 20, 2007

The most critical part of dioxygen evolution in photosystem II is the O−O bond formation step. In order to reach an efficient mechanism, nature uses a unique oxygen-evolving complex (OEC) having four manganese and one calcium center. Even though the structure of the OEC has become much more clear during recent years, it has still been difficult to find a transition state (TS) for O−O bond formation with a sufficiently low barrier. However, about a year ago, a quite surprising type of TS was found. With the latest X-ray ligand assignment, the local barrier for this TS is only 5.1 kcal/mol. It can be described as an attack by an oxygen radical, held by a dangling manganese, on a bridging oxo ligand in the Mn_3Ca cube. In the present short Article, energy diagrams describing the entire process of dioxygen formation will be presented. An important conclusion drawn from these diagrams is that the major features of dioxygen formation remain the same irrespective of which one of the experimentally suggested structures the diagram is built on. Compared to earlier presentations of the same type, a slightly different approach has been used for setting up the diagrams. Results from a recent experimental study of the pressure dependence of oxygen release have been used to define the final energy levels. The loss of energy in the electron transfer from Tyr_z to P_{680} has also been incorporated into the diagrams. A good agreement with experimental observations is demonstrated.

Introduction

An X-ray structure has been the starting point for essentially all quantum chemical studies of enzymatic mechanisms. This structure has to contain the main features but does not have to be very accurate. Because several intermediates are generally needed in the study of a mechanism, bond distances and angles always have to be optimized anyway, to produce a comparable set of energies. Furthermore, because the mechanism depends on the energetics, which is rather insensitive to details of the structures, a rather low level of optimization is needed in practice. Still, without the main features of the structure as a starting point, a quantum chemical study becomes very tedious and often impossible in practice. Because the first quantum chemical studies of dioxygen evolution in photosystem II (PSII) were initiated before any X-ray structure of the oxygen-evolving complex (OEC) was available,[1,2] they had to rely on more general information. At that stage, EXAFS information of Mn−Mn distances in different *S* states was particularly important.[3] A model with two manganese and a calcium connected by μ-oxo bonds in a cube could be set up. There was not enough information to suggest the position for all manganese atoms, and one of them was therefore left out of the model. Furthermore, as it later turned out, the third manganese and calcium were misplaced. The main result of those studies was that the formation of an oxygen radical ligand appears to be critical for O−O bond formation. O−O bond formation was suggested to occur by an attack of a second-sphere water on the oxygen radical.

Significantly better possibilities to obtain accurate information from calculations concerning the OEC mechanism

* E-mail: ps@physto.se. Telephone: +46-8-16 12 63. Fax: +46-8-55 37 86 01.

(1) Siegbahn, P. E. M.; Crabtree, R. H. *J. Am. Chem. Soc.* **1999**, *121*, 117–127.
(2) Siegbahn, P. E. M. *Inorg. Chem.* **2000**, *39*, 2923–2935.
(3) Yachandra, V. K.; Sauer, K.; Klein, M. P. *Chem. Rev.* **1996**, *96*, 2927–2950.

10.1021/ic7012057 CCC: $40.75
Published on Web 03/10/2008

appeared when the first X-ray structures became available. Zouni et al. were the first to obtain crystals that defract at reasonable, although low, resolution of 3.2–3.8 Å.[4] From their analysis, relative positions of the four manganese centers could be suggested. Similar information was obtained from a later X-ray structure by Kamiya and Shen.[5] Still, the positioning of calcium was not clear, and the amino acid ligands could not be assigned. A major step forward came a few years later when Ferreira et al. were able to assign also the position of calcium in the OEC as well as the general shape of the complex, even though the resolution was still low at 3.5 Å.[6] A cube formed by three manganese and calcium connected by μ-oxo bonds with the fourth manganese outside the cube was suggested from their analysis, which also makes use of previous results from EXAFS.[3] A reasonable assignment of the ligand structure around the OEC was also made for the first time. Recently, a new X-ray analysis by Loll et al.,[7] based on a slightly higher resolution of 3.0 Å, confirmed the general structure of the OEC. Interesting modifications of the structure were also suggested from their analysis.

Even though a much better starting point for the computational studies was obtained with the new X-ray structure, progress on the mechanism has been rather slow. It took years of computations to realize that the fourth manganese is probably farther out from the Mn_3Ca cube than initially suggested,[8] Better results were also obtained when the bicarbonate, originally placed between calcium and the outer manganese, was removed.[9] Both of these findings came parallel to the most recent X-ray analysis, which also suggests these modifications of the original structure.[7]

Another important development toward an understanding of the mechanism occurred when it was realized how accurate redox potentials and pK_a values could be obtained from calculations on small models of the OEC.[9] By a simple adjustment of the computed results to the known driving force for the catalytic cycle, the main features of an energy diagram containing all of the *S* transitions could be obtained. By minimization of the energy barriers, a complete energy diagram can also be constructed without explicit consideration of the actual enzyme surrounding the OEC. It only has to be assumed that the surrounding enzyme stays essentially the same in all *S* transitions.

The main result obtained so far from model calculations came after a systematic investigation of essentially all possible pathways of O−O bond formation, starting from the best S_4 state obtained.[8] As in all previous computational studies, the lowest barrier for O−O bond formation was found for a state that contains an oxygen radical. However, unlike the earlier studies, and very surprisingly, the lowest barrier was found for an attack of the oxygen radical on a bridging oxo ligand in the Mn_3Ca cube. This was very surprising because these oxo ligands were considered quite inert and strongly bound to the OEC. As the O−O bond is formed, the bond between the oxo ligand and the rest of the cube has to be substantially weakened, and it was hard to realize that this would be possible without creating a high barrier. The explanation was that all of the other Mn−oxo and Ca−oxo bonds were strengthened in the process, compensating for the loss of bonding to the oxo forming dioxygen.

So far, there has been essentially only one other computational attempt to find the mechanism of dioxygen formation in PSII.[10] In that approach, a large portion of the protein was incorporated into the model using the quantum mechanical/molecular mechanics (QM/MM) method. The X-ray structure of Ferreira et al. was used as a starting point for the geometry optimizations. The analysis was focused on one type of mechanism suggested earlier based on experiments.[11] QM/MM is a much more cumbersome approach than the one used in the present study, and for this reason, no redox potentials, pK_a values, or transition states (TSs) were computed. General arguments, rather than the energies obtained from the QM/MM approach, were used to test whether the mechanism was plausible. If more experimental structural information had been available for intermediates at the stage at which the O−O bond was formed, this approach might be more predictive, but in the near future, such information does not seem to be possible to obtain because of the short-lived nature of these intermediates.

In the present short Article, the above-mentioned results will be discussed, also including some new insights concerning the mechanism for O−O bond formation. Full mechanisms and energy diagrams will be presented for most of the recent structural suggestions, including the original structure by Ferreira et al. and the more recent structure by Loll et al., and finally for a few of the structures recently suggested based on EXAFS.[12] Investigations of the effect of a chloride ligand, and the effects of substituting calcium with cadmium or strontium will be described. The results are surprisingly accurate compared to experiments, particularly when the ligand assignment of the most recent X-ray structure is used.

Methods

The calculations discussed here were made using the density functional theory (DFT) hybrid functional B3LYP,[13] with procedures very similar to those used in previous studies.[8,9,14,15] Small

(4) Zouni, A.; Witt, H.-T.; Kern, J.; Fromme, P.; Krauss, N.; Saenger, W.; Orth, P. *Nature* **2001**, *409*, 739–743.
(5) Kamiya, N.; Shen, J.-R. *Proc. Natl. Acad. Sci. U.S.A.* **2003**, *100*, 98–103.
(6) Ferreira, K. N.; Iverson, T. M.; Maghlaoui, K.; Barber, J.; Iwata, S. *Science* **2004**, *303*, 1831–1838.
(7) Loll, B.; Kern, J.; Saenger, W.; Zouni, A.; Biesiadka, J. *Nature* **2005**, *438*, 1040–1044.
(8) Siegbahn, P. E. M. *Chem.—Eur. J.* **2006**, *12*, 9217–9227.
(9) Siegbahn, P. E. M.; Lundberg, M. *J. Inorg. Biochem.* **2006**, *100*, 1035–1040.
(10) Sproviero, E. M.; Gascon, J. A.; McEvoy, J. P.; Brudvig, G. W.; Batista, V. S. *J. Chem. Theor. Comput.* **2006**, *4*, 1119–1134. *Curr. Opin. Struct. Biol.* **2007**, *17*, 173–180.
(11) Vrettos, J. S.; Stone, D. A.; Brudvig, G. W. *Biochemistry* **2001**, *40*, 7937–1945 , with corrections in *Biochemistry* **2003**, *42*, 848.
(12) Yano, J.; Kern, J.; Sauer, K.; Latimer, M. J.; Pushkar, Y.; Biesiadka, J.; Loll, B.; Saenger, W.; Messinger, J.; Zouni, A.; Yachandra, V. K. *Science* **2006**, *314*, 821–825.
(13) Becke, A. D. J. *Chem. Phys.* **1993**, *98*, 5648–5652.
(14) Lundberg, M.; Siegbahn, P. E. M. *Phys. Chem. Chem. Phys.* **2004**, *6*, 4772–4780.

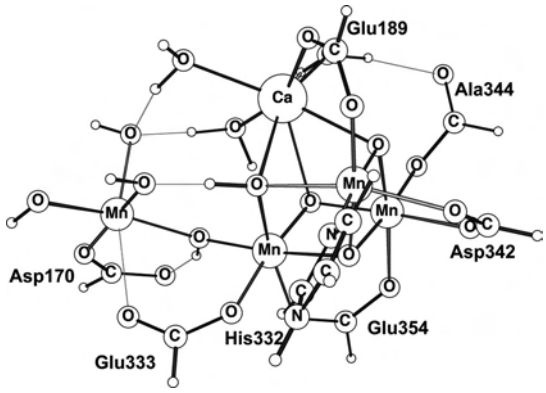

Figure 1. Optimized $S^{-1}{}_1$ state for a model based on the most recent X-ray structure.[7]

basis sets for the geometries (lacvp), large basis sets for energies [cc-pvtz(-f)], and a surrounding dielectric medium with a dielectric constant equal to 4.0 were used (basis lacvp*). The performance of the B3LYP functional for the present type of problems has recently been reviewed,[16] indicating a typical accuracy within 3–5 kcal/mol, normally overestimating barriers. A procedure different from that used by other workers for obtaining redox potentials and pK_a values is a key feature of the present approach.[9,15,17–20] Using experimental information about the driving force and a single adjustable parameter, it is possible to determine accurate values for these properties without explicitly describing the enzyme surrounding the active site. The results are essentially independent of the choice of the dielectric constant. The calculations were performed with the programs *Jaguar*[21] and *Gaussian03*.[22] A typical chemical model used in the calculations is shown in Figure 1.

Results

Energy Diagrams. The most important step in the dioxygen evolution mechanism is obviously when the O−O bond is formed. The details of a recent suggestion of how this is made will be described below. However, to fully describe dioxygen evolution, the energetics of all steps preceding and following the O−O bond formation are also needed. The thermodynamics of these steps depend on the redox potentials of the manganese atoms of the OEC for all of the *S* states, and of the pK_a values of the water-derived ligands, because both electrons and protons are removed from the complex. It will here be assumed that the electrons and protons are removed in an alternating fashion to avoid charge buildup. The total charge of the OEC will still have to change but not by more than one unit. For the present models, it will alternate between −1 and 0.

When an energy diagram containing most features of O−O bond formation is constructed, the total driving force for the full catalytic cycle is a key factor. This value can be obtained from known redox potentials. In the case of water oxidation in PSII, the redox potential of the donor O_2/H_2O is 0.8 V, and for the ultimate acceptor $P^+{}_{680}$, it is 1.3 V.[23,24] The driving force therefore becomes 4(1.3 − 0.5) eV = 46 kcal/mol. This is the value used in recent presentations of mechanistic energy diagrams.[25] However, it could be argued that Tyr_z rather than $P^+{}_{680}$ is the acceptor of the electrons from the manganese cluster and that the redox potential of Tyr_z should be used in the expression for the driving force. Tyr_z is situated between the OEC and P_{680} in the X-ray structure, about 5 Å away from the OEC and 10 Å away from P_{680}.[6] The exact redox potential of Tyr_z is not known, but in order not to waste energy, the redox potential of Tyr_z should ideally be the same as that of P_{680}. If this was the case, the choice of acceptor would not matter. However, the mere fact that the Tyr_z radical is observable means that its redox potential should be slightly smaller than that of P_{680}.[26,27] In the present derivation of mechanistic energy diagrams, it is assumed that the redox potential of Tyr_z is 3 kcal/mol smaller than that for P_{680}, and this energy is thus lost for each photon absorption. With four photon absorptions, this means that the actual driving force used by the OEC for making dioxygen should be 46 − 4(3) = 34 kcal/mol, and this will be the value used for the present diagrams. The most probable reason that the enzyme is prepared to sacrifice as much as 12 kcal/mol (for each dioxygen formed) when $P^+{}_{680}$ is reduced could be to secure the charge separation in the reaction center. Another major role of Tyr_z is to make electron transfer between the manganese cluster and P_{680} unidirectional, preventing shortcuts. The role of Tyr_z as a hydrogen abstractor[28] is unlikely based on energetic consideration.[25]

As mentioned above, both redox potentials and pK_a values of the OEC are needed to construct a complete energy diagram. These values are very difficult to obtain from the present types of models having only a modest number of atoms (less than 100). When a system changes its charge, there will be a large long-range response that would require a much more extended model to describe. The size of this response is typically on the order of 20–25 kcal/mol. However, if both a proton and an electron (an H^+/e^- couple) are removed from the complex, the response from the surrounding will be much smaller, on the order of only a few kilocalories per mole. Simple dielectric cavity models,

(15) Siegbahn, P. E. M.; Lundberg, M. *Photochem. Photobiol. Sci.* **2005**, *4*, 1035–1043.
(16) Siegbahn, P. E. M. *J. Biol. Inorg. Chem.* **2006**, *11*, 695–701.
(17) Siegbahn, P. E. M. *Adv. Inorg. Chem.* **2004**, *56*, 101–125. Siegbahn, P. E. M.; Tye, J. W.; Hall, M. B. *Chem. Rev.* **2007**, in press..
(18) Siegbahn, P. E. M.; Blomberg, M. R. A. *J. Phys. Chem. B* **2003**, *107*, 10946–10955. Blomberg, M. R. A.; Siegbahn, P. E. M. *J. Comput. Chem.* **2006**, *27*, 1373–1384.
(19) Blomberg, L. M.; Blomberg, M. R. A.; Siegbahn, P. E. M. *Biochim. Biophys. Acta* **2006**, *1757*, 31–46. Blomberg, L. M.; Blomberg, M. R. A.; Siegbahn, P. E. M. *Biochim. Biophys. Acta* **2006**, *1757*, 240–252. Blomberg, L. M.; Blomberg, M. R. A.; Siegbahn, P. E. M. *J. Biol. Inorg. Chem.* **2007**, *12*, 79–89.
(20) Siegbahn, P. E. M.; Shestakov, A. F. *J. Comput. Chem.* **2005**, *26*, 888–898.
(21) *Jaguar*, 5.5; Schrödinger LLC: Portland, OR,1991–2003.
(22) Frisch, M. J.; et al. *Gaussian 03*, revision B.03; Gaussian Inc.: Pittsburgh, PA, 2003.
(23) Diner, B. A. *Biochim. Biophys. Acta* **2001**, *1503*, 147–163.
(24) Rappaport, F.; Lavergne, J. *Biochim. Biophys. Acta* **2001**, *1503*, 246–259.
(25) Siegbahn, P. E. M. *Proc. R. Soc. London*, in press.
(26) Brettel, K.; Schlodder, E.; Witt, H. T. *Biochim. Biophys. Acta* **1984**, *766*, 403–415.
(27) Renger, G. *Biochim. Biophys. Acta* **2004**, *1655*, 195–204.
(28) Hoganson, C. W.; Lydakis-Simantiris, N.; Tang, X.-S.; Tommos, C.; Warncke, K.; Babcock, G. T.; Diner, B. A.; McCracken, J.; Styring, S. *Photosynth. Res.* **1995**, *46*, 177.

as used here, are normally able to describe the effects of this size rather accurately. To obtain the absolute energies needed to remove an H^+/e^- couple, use is made of the total driving force of 34 kcal/mol, as derived above. In practice, this means that every second energy level in the energy diagrams should be rather accurately described with a model of a limited size. This should also be true for the local barrier of O−O bond formation, which together with these energy levels constitutes the main features of the energy diagram describing the mechanism of O−O bond formation. It also means that evolution of the enzyme surrounding the OEC should not have been able to significantly modify these features of the mechanism. On the other hand, they will depend critically on the structure of the OEC itself.

For a complete energy diagram, all relevant redox potentials and pK_a values are needed. Because accurate values are very difficult to calculate for these entities, as described above, they will instead be obtained from the use of a single adjustable parameter. A single parameter is sufficient with the assumption that the enzyme surrounding the enzyme is the same in all transitions and would therefore give the same response when a charge is removed at all stages of the mechanism. The parameter will be fitted to make the *S*-state transitions exergonic, as required by experiments, and to minimize the barriers between the transitions. The latter aspect is where evolution has entered and optimized the function of the enzyme. The single parameter mimics this evolution.

One more aspect of the construction of the energy diagrams has to be discussed before they are presented. This concerns the final step of the diagram where dioxygen is released and two water molecules become bound to the OEC. This is probably the most difficult part to model accurately at present because the details of the structure are not yet firmly established and major structural changes are involved. Still, in the previous energy diagrams,[25] an attempt was made to calculate this energy. The results will be briefly mentioned here. For the present diagrams, another approach is used. Recently, the pressure dependence of the oxygen release has been studied experimentally.[29] An interesting result of that study is the finding of an intermediate preceding the release. It is here suggested that the intermediate observed is the bound peroxide, formed directly after O−O bond formation. The alternative that the intermediate should be a state prior to O−O bond formation is much less likely because this would imply that the stability of the intermediate would be sensitive to the membrane gradient. In the experiment, it was also found that the intermediate has very nearly the same energy as the final product after oxygen release. This finding is used for the present diagrams by setting the bound peroxide at the same energy (−34 kcal/mol) as the final product. With this modification of the strategy and also the use of a different driving force, the present energy diagrams will be slightly different from those presented previously,[25] even though they are based on the same calculations for the same structures.

(29) Clausen, J.; Junge, W. *Nature* **2004**, *430*, 480–483.

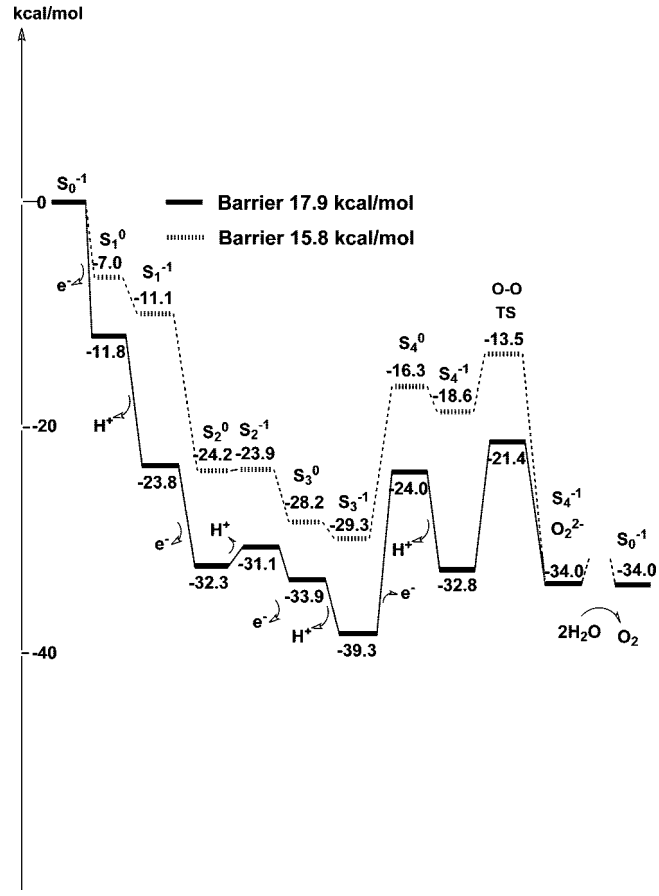

Figure 2. Energy diagrams for dioxygen evolution in PSII. The full bars correspond to the ligand assignment from the first X-ray structure,[6] while the hashed bars correspond to the latest one.[7]

The diagrams, constructed as described above, for the ligand assignment of both the first[6] and latest[7] X-ray structures are shown in Figure 2. It should be noted in this context that, in the case of the first X-ray structure, the bicarbonate has been removed[9] and the dangling manganese has been placed farther out than originally suggested.[8] Otherwise, the barrier for O−O bond formation would have been much higher. The states in the diagram are labeled $S^q{}_n$, where the lower index denotes the *S* state and the upper index the charge of the model. In a transition between $S^0{}_n$ and $S^{-1}{}_n$, a proton is thus released, while in a transition between $S^{-1}{}_n$ and $S^0{}_{n+1}$, an electron is released. The main features of the two curves in the figure are quite similar. The two first *S*-state transitions are strongly exergonic, more so for the first X-ray structure than for the latest one, however. The S_2 to S_3 transition is only weakly exergonic. The most interesting development starts after the $S^{-1}{}_3$ state has been reached. For both structures, there is a strongly endergonic transition leading to the $S^{-1}{}_4$ state, involving both an endergonic electron release and an exergonic proton release. The overall rate-limiting barrier should be counted from the resting state at $S^{-1}{}_3$ to the TS for O−O bond formation in the $S^{-1}{}_4$ state. This barrier for the latest X-ray structure is then 29.3 − 13.5 = 15.8 kcal/mol, while the one for the first structure is 39.3 − 21.4 = 17.9 kcal/mol, indicating that the latest X-ray structure is probably a slightly better representation of the actual OEC because it has a lower overall barrier. The

experimental turnaround time in milliseconds indicates a rate-limiting barrier of 13–14 kcal/mol. The results for both of these X-ray structures are thus surprisingly accurate considering the remaining uncertainties in the ligand assignments. An overestimation of a barrier by a few kilocalories per mole is quite normal when the hybrid functional B3LYP is used. As mentioned above a new strategy has been used for the final step of the mechanism, where the bound peroxide is placed at the same energy as that for the final product. In attempts to actually calculate the energy for this transition, the result for the latest X-ray structure gave an exergonicity of −7.6 kcal/mol, while for the earlier one, an exergonicity of −8.9 kcal/mol was obtained. This estimate is, for example, built on an assumed binding energy of a water molecule in bulk water of 14 kcal/mol. Because the transition energy for the final transition should be close to zero, there is a slight error in these estimates, which could be due to the structures used but perhaps more probably due to the uncertainties in the way the energies are calculated. An important result, demonstrated by the diagrams in Figure 2, is that the rate-limiting barrier for O−O bond formation is determined not only by the local O−O bond formation but also by the endergonicity of the preceding S_3 to S_4 transition. This means that, even though the difference between the local O−O barriers for the two structures is 11.4 − 5.1 = 6.3 kcal/mol, the difference between the rate-limiting barriers is only 2.1 kcal/mol. Another interesting conclusion is that a proton release is included in the rate-limiting step, which means that the barrier will increase by at least 4.1 kcal/mol (3 pH units) for the full membrane gradient.

Structures Based on EXAFS. Recent EXAFS studies have led to the conclusion that there are three Mn−Mn vectors in the range 2.7–2.9 Å in the S_1 state of the OEC.[30] The optimized geometries for the structures discussed above, based on the two X-ray structures, have only two short Mn−Mn vectors, indicating possible remaining problems in the structures. The reason for this is that one of the oxo ligands in the Mn_3Ca cube becomes protonated in both types of structures. This occurs because the pK_a values for these ligands become quite high. It is thus important to emphasize that the general structure adopted for the OEC does not by itself determine the number of short Mn−Mn distances, but the protonation states of the bridging ligands are at least as important. Another indication that the structures suggested by the different X-ray structures are not entirely correct is that the shifts of the computed IR frequencies for the ligand carboxylates[25] do not match experimental observations[31,32] for the above types of structures. Alternative structures are therefore still of high interest, even though the X-ray structures may capture the main features correctly. The most recently suggested structures attempt to combine EXAFS and X-ray crystallography.[12] These structures have also been used

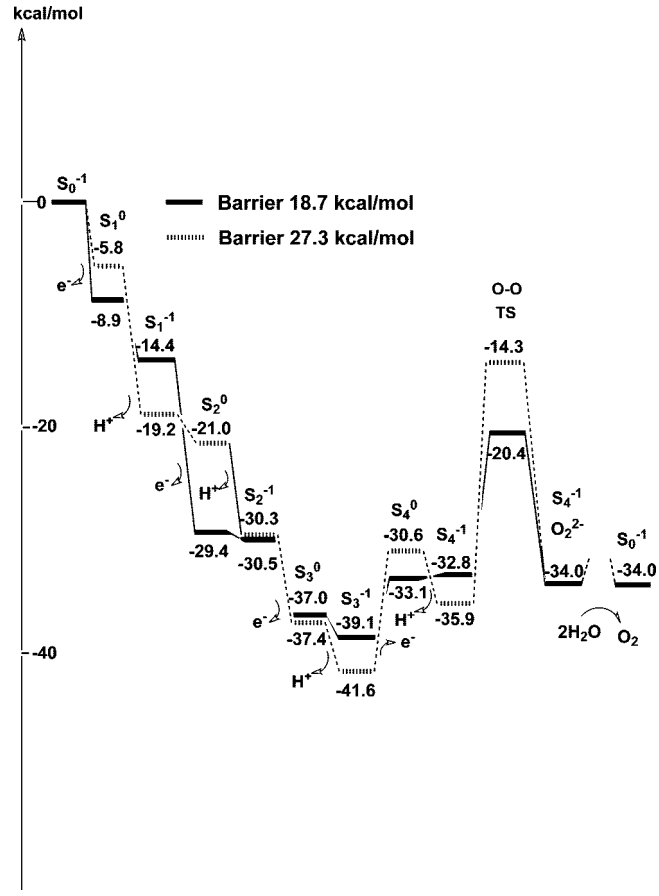

Figure 3. Energy diagrams for dioxygen evolution in PSII. The full bars correspond to structure III suggested by EXAFS, while the hashed bars correspond to structure IIa.[10]

here in a construction of complete energy diagrams. Only two of the four types of structures suggested in detail could be carried all the way to full diagrams (see Figure 3). For the structure labeled I in the EXAFS study, it was too difficult at present to assign reliable positions for the ligands, and the optimizations of structure II converged to the same geometries as those based on structure IIa. For IIa, an investigation similar to the one described above led to structures with protonations of two of the bridging oxo ligands (see Figure 4), which meant that the optimizations failed to reproduce three short Mn−Mn distances for this type of structure. Also, the computed rate-limiting barrier for IIa is 27.3 kcal/mol, much higher than those for the X-ray structures. The most interesting structural results were instead obtained for structure III, where it was actually possible to retain three short Mn−Mn distances from S_0 through S_3, even though one of the bridging oxo ligands became protonated (see Figure 4). Apparently, the Mn−Mn distances are less sensitive (only 0.05 Å) to protonations of the oxo ligands bridging to the outer manganese (the one most to the left in the figure) than they are to protonations of the oxo ligands in the Mn_3Ca part of the OEC. The energetics (obtained in the same way as above) with a rate-limiting barrier of 18.7 kcal/mol is not as close to experiments as that obtained for the X-ray structures in Figure 2. It is in this context important to note that part of the reason the overall barrier is still quite reasonable is that the experimental energetics was used for

(30) Yano, J.; Pushkar, Y.; Glatzel, P.; Lewis, A.; Sauer, K.; Messinger, J.; Bergmann, U.; Yachandra, V. *J. Am. Chem. Soc.* **2005**, *127*, 14974–14975.
(31) Chu, H.-A.; Hillier, W.; Debus, R. J. *Biochemistry* **2004**, *43*, 3152–3166.
(32) Debus, R. J.; Strickler, M. A.; Walker, L. M.; Hillier, W. *Biochemistry* **2005**, *44*, 1367–1373.

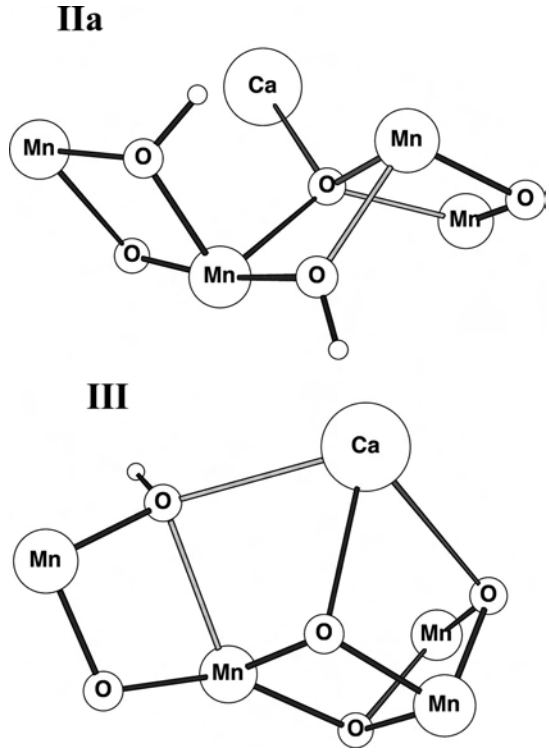

Figure 4. Type IIa and III structures suggested by EXAFS for the $S^{-1}{}_1$ state. Only the metal atoms and the oxo bridges are shown for clarity.

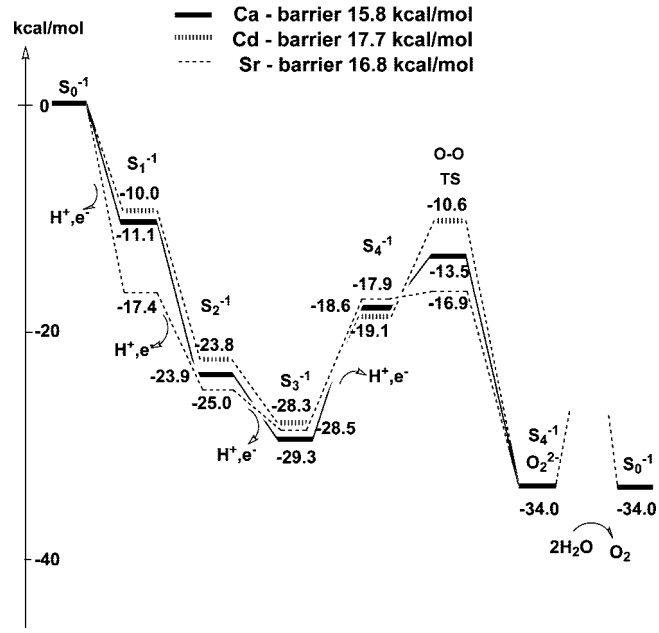

Figure 5. Energy diagrams for dioxygen evolution in PSII. The full bars correspond to a complex with calcium, the hashed bars to cadmium, and the dashed bars to strontium. Only every other transition is shown for clarity. Note that the lowest point before O−O bond formation in the case of strontium is $S^0{}_3$ at –33.7 kcal/mol (not shown).

the final step. In the previous study, where the energetics of the final step was calculated, the resulting energy diagram was much worse.[25] The final step was computed to be exergonic by as much as 26.2 kcal/mol for structure III when it should be close to zero, indicating that there are still substantial problems with this structure. A major reason for this is that it is too difficult to make the required reduction of the manganese center in the O−O bond formation step because it is surrounded by three negative oxo ligands and two carboxylates. The driving force in this critical step therefore becomes too low. This error in the description is thus hidden by the use of the experimental energetics for the final step. Therefore, it still probably remains to find another ligand assignment that is different from the ones suggested so far, giving agreement with the EXAFS interpretations and a better picture of the energetics. Another possibility is that a different type of TS for O−O bond formation could be found for this structure. At present, the search for different TSs has not been as thorough as that for the X-ray structures. However, given the quite strict requirements for an optimal TS for O−O bond formation, as described below, it is at present hard to see how the TS could be very different from the ones found for the X-ray structures and still give a low barrier.

Effects of Cadmium, Strontium, and Chloride. An interesting test of a mechanism and the structures is to investigate the effects of substituting calcium with cadmium or strontium and of adding chloride. Cadmium is usually considered to be the metal that most strongly resembles calcium, and it is therefore somewhat surprising that replacement of calcium by cadmium prevents dioxygen formation.[11] The calculations on cadmium, performed for the structure based on the most recent X-ray structure, confirm the picture that it is very similar to calcium with energy diagrams that do not differ very much, see Figure.5. For clarity, only every second state is shown in the diagram. The rate-limiting barriers found are 15.8 kcal/mol for calcium and 17.7 kcal/mol for cadmium, which may be enough to explain the experiments. For strontium, the individual steps differ much more, but the rate-limiting barrier of 16.8 kcal/mol is only 1.0 kcal/mol higher than the one for calcium of 15.8 kcal/mol. This result is consistent with the observation that strontium is still active, but with a lower overall rate. However, it should be remembered that the accuracy of the calculations is hardly enough to draw definite conclusions about rates with so similar barriers. A quite interesting result for strontium is that the local barrier for O−O bond formation was found to be only 1.0 kcal/mol, which is remarkably low. Still, because the overall rate-limiting barrier also contains the endergonicity for forming the $S^{-1}{}_4$ state, the rate will be slower than that for calcium.

The effects of chloride are also found to be very small. The optimal position for chloride was found to be on the dangling manganese. This result is different from a recent QM/MM study, where chloride was suggested to be ligated to calcium.[10] An explanation for this difference could be that the present position for chloride was determined on energetic grounds, while in the other study, the position was determined on structural grounds. The present energetic comparison with and without chloride becomes slightly parameter-dependent. As discussed above, a parameter has to be chosen to construct the diagrams, and this parameter is set to minimize the barriers involved. It could be considered as a parameter for the optimal enzyme surrounding the OEC. If optimal parameters are used both with and without chloride,

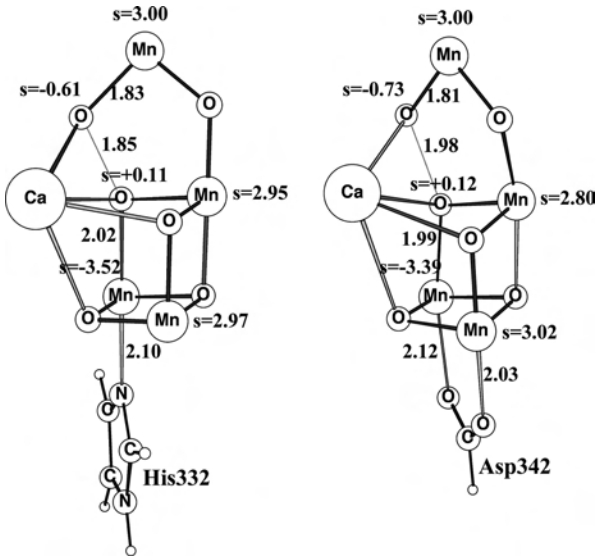

Figure 6. Optimized TSs for O−O bond formation. The structure based on the first X-ray structure[6] is shown to the left, and the one based on the most recent analysis[7] is shown to the right. Only the most important atoms are shown for clarity. Distances are in angstroms, and spin populations are given.

the barrier becomes 1.2 kcal/mol lower without chloride. However, it could be argued that if chloride is present in the actual cluster, the environment should be optimized for chloride. Therefore, if the optimal parameter for chloride is used also for the case without chloride, the barrier is 1.9 kcal/mol lower with chloride. Again, the main conclusion drawn is that the results are very similar, with the differences being too small to draw firm conclusions.

Requirements for a Low O−O Bond Formation Barrier. An entirely new type of TS for O−O bond formation was found about 1 year ago.[8] This TS is shown in Figure 6 for both the old and new ligand assignment. Only the most important atoms are shown for clarity. The model used, shown in Figure 1, is the same as the one for the other results described here. The local barrier for the one based on the most recent X-ray structure is only 5.1 kcal/mol, compared to 11.4 kcal/mol for the original structure. As in earlier studies, an oxygen radical is a key component of the O−O bond formation mechanism. In relation to earlier studies, the most surprising feature of the TS is that O−O bond formation occurs by an attack of this oxygen radical on a bridging oxo ligand in the Mn_3Ca cube. Earlier studies had instead indicated a reaction between the oxygen radical and a second-sphere water molecule, but this type of TS had a much higher barrier of 20 kcal/mol.

There are several important features of the new TS, described in detail in earlier studies.[8,25] The first requirement for a low barrier is that the spins on the atoms involved are alternating. The reason for this is partly obvious. If the oxygen radical has a down spin, as in the figure, it is clear that it should form a bond with an oxygen which has an up spin. Therefore, the electron transferred from the oxo ligand to the manganese in the cube has to have a down spin, with the up spin on the electron remaining on the oxo ligand. Because a high-spin configuration is the ground state of all manganese states, the manganese in the cube receiving the electron has to have all of its d electrons with down spins. This explains the sequence of spins on the oxygen radical, the oxo ligand, and the manganese in the cube. The least obvious spin requirement for a low barrier is that the dangling manganese should have an up spin. One reason for this is that an antiferromagnetic coupling between the dangling manganese and the oxygen radical is a few kilocalories per mole lower than the ferromagnetic coupling for the reactant, because of the introduction of some double-bond character. Also, the alternating alignment of the spins in the figure is a requirement if the ground state of the reactant should go smoothly over to the ground state of the product, without crossing to another surface, but the energetic effect on the barrier is surprisingly large.

Another important requirement for a low barrier is that the manganese in the cube should be easily reduced to manganese(III) in the step where the O−O bond is formed. This leads to a few requirements for the ligands on this manganese. First, because manganese(III) is Jahn–Teller (JT) active, a good JT axis has to be available. Also, because the bond between this manganese and the oxo ligand becomes broken in the O−O bond formation process, the JT axis has to point along this Mn−O bond. With the first X-ray assignment of the ligands, His332 is placed opposite to the Mn−O bond, which is good because histidine is a neutral ligand and can therefore easily extend its bond length to manganese. A negative monodentate carboxylate would have a much stronger bond to manganese and would therefore be a significantly less optimal ligand along the JT axis. However, a bidentate ligand, like Asp342 in the most recent X-ray structure, is even better because its loss of binding to manganese(III) can be compensated for by a strengthening of its bond to the other manganese (see the figure). An easy reduction of manganese also puts important demands on the charges of the ligands on this center. For the new X-ray structure, this manganese has unusually few negative ligands and is therefore easily reduced, leading to a strong driving force for O−O bond formation of 15.4 kcal/mol and a low local barrier of 5.1 kcal/mol (see Figure 2). In contrast, the driving force for the original X-ray structure is only 1.2 kcal/mol and the local barrier therefore much higher with 11.4 kcal/mol. It is possible that the character of the ligands on the manganese being reduced is a more important factor for a favorable O−O bond formation than earlier realized. Undoubtedly, the rather high barriers for the EXAFS-derived structures depend on a poor ligand environment for this manganese. New suggestions of ligands on this center could therefore improve the situation.

Summary

The rate-limiting barrier for O−O bond formation is experimentally 13–14 kcal/mol. For a long period, after years of DFT investigations, the lowest barrier found was around 20 kcal/mol.[9,14,15] In that mechanism, the O−O bond was formed in a reaction between an oxygen radical and a second-sphere water molecule. Because the local O−O bond formation barrier was already so high, it was concluded that

the oxygen radical reactant should be formed without additional cost. A finding of an entirely different TS with a much lower barrier of 11.4 kcal/mol completely changed this scenario.[8] With the most recent ligand assignment of the OEC,[7] the local barrier decreased even further to 5.1 kcal/mol. The TS can be described as an attack of an oxygen radical, held by the dangling manganese, on an oxo ligand in the Mn_3Ca cube. This was a very surprising result because the bridging oxo ligands were supposed to be quite inert. With such a low barrier as 5.1 kcal/mol, the conclusion that the S_4 reactant should be reached without cost could be reevaluated. Instead, in the mechanism presented here, the reactant is reached in a quite endergonic step composed of both an electron and a proton release. The sum of this endergonic process and the local O−O bond formation barrier then makes up the total barrier for the rate-limiting step. The computed value for the most recent ligand assignment is 15.8 kcal/mol, quite close to the experimental 13–14 kcal/mol range.

The goal of a theoretical study of the mechanism for O−O bond formation in PSII is to present an energy diagram including all *S*-state transitions, the O−O bond formation step, and the final dioxygen release. The latter step is quite difficult to study by the present methods because it involves both an uptake of two water molecules from the bulk and a release of oxygen, including an entropy gain. Furthermore, the result will depend critically on the structure, which still has uncertainties. Therefore, in the present study, a different approach has been used. The pressure dependence of oxygen release has recently been studied experimentally,[29] and it was concluded that the final process going from a yet unidentified intermediate to the final dioxygen product is essentially thermoneutral. By identification of the unknown intermediate with the bound peroxide formed directly after O−O bond formation, this experimental information could be used here in the construction of an energy diagram by placing the peroxide at the same energy as the final product. The final product is placed at −34 kcal/mol, which is the computed driving force assuming a loss of 3 kcal/mol in the electron transfer between Tyr_z and P_{680}. This leads to slightly different energy diagrams different from those presented earlier.[25] The overall energetics obtained is in good agreement with experimental information, but there are several results indicating structural disagreements, which means that alternative structures for the OEC will continue to be of high interest for future model studies.

A major conclusion drawn from the present diagrammatic analysis of dioxygen formation in PSII is that the main features remain the same irrespective of which structure the diagram is built on (see Figures 2, 3, and 5). These main features are three relatively exergonic and easy transfers from S_0 to S_3. The electron transfer from S_3 to S_4 is instead quite endergonic, generating a key oxygen radical bound to one of the manganese atoms. In S_4, the optimal O−O bond formation occurs in the same way for all structures, by an attack of the oxygen radical on a bridging oxo ligand in the Mn_3Ca cube.

A natural next step in the present approach is to build more of the structural information available from X-ray crystallography into the models. This can be done by constraining certain atoms to remain at the experimentally suggested positions and by extending the model with longer side chains and with amino acids outside the OEC core. These types of calculations are presently underway. At the present stage of these calculations, the main features of O−O bond formation, as described above, remain the same. However, there is a marked sensitivity to the structural strain as to which manganese center is oxidized and to which group is deprotonated in the earlier *S* transitions. It should in this context be noted that the strain introduced could be partly artificial because of the low resolution of the X-ray structures available. Still, results of this type could shed new light on the accuracy of the present predictions.

IC7012057